DOI: 10.14529/power190202

EXPERIMENTAL INVESTIGATION OF HYDRODYNAMICS AND HEAT TRANSFER CHARACTERISTICS OF TWO-PHASE GAS/LIQUID MIST FLOW IN TANDEM ARRANGED HEATED SPHERES

Akram H. Abed[1, 2], *akraaam82@yahoo.com,*
S.E. Shcheklein[1], *s.e.shcheklein@urfu.ru,*
V.M. Pakhaluev[1], *valer-1939@mail.ru*
[1] *Ural Federal University named after the first President of Russia B.N. Yeltsin, Ekaterinburg, Russian Federation,*
[2] *University of Technology, Baghdad, Iraq*

The article presents an experimental investigation, performed to evaluate the hydrodynamics and heat transfer characteristics in tandem arranged heated rows packed inside cylindrical channel, which use air as well as air/water mist flows as operational medium. The average surface temperature has been recorded under various air main flow, water mist rate, surface heat flux and constant pitch ratio (y/d = constant). The heat transfer rate was found to increase with the water mist rate and decrease with the surface temperature. Heat transfer rate was enhanced over that for the single-phase air flow as a result of water mist evaporation and direct heat conduction by the water film generated on the heated surfaces. Overall, the heat transfer coefficient was enhanced by about 140%, 42%, and 10% respectively for the upper, middle and lower heated rows by suspending (111.68 kg m^{-2} hr^{-1}) water mist rate. The frictional resistance for air/water mist flow is found to exceed that in the single-phase air flow. Compared to each water mist rate over the investigated range, the percentage enhancement in the overall heat transfer performance factor of around 116%, 35%, and 10% respectively for all the heated rows under the highest water mist rate. New experimental results obtained can be used in the development of heat exchanger modules design processes.

Keywords: experimental investigation, mist flow, heat transfer enhancement, tandem arrangement, water film.

Introduction

In air/water mist cooling process, the water mist carried by the main air flow hits the first row of heating surface located upstream. In order to enhance the heat transfer process using the latent evaporation heat, the heating surface should be covered with a water film, as wide and as thin as possible. That means that the water mist must be extended to the heated surface located in other rows of heat exchange devices [1, 2]. The investigations of air/water mist cooling have widely covered the heating surfaces with an active water droplet impingement. As for a single heated cylinder, Lee et al. [3] have performed experimental investigations and quantitative analysis on air/water mist cooling in a horizontal cylinder. Furthermore, Kosky et al. [4], Kuwahara et al. [5] have performed experimental studies using a roughened cylinder to enhance the wettability of the heated surface. As for the heat transfer from a stack of spheres exposed to air/water mist two-phase flow, Allais et al. [6, 7] conducted such experiments with low airflow velocity, low water mass flow rate, and limited ranges of temperature difference. For mist-cooled heat exchanger, Yang et al. [8], Treble [9], Song et al. [10] and Deshmukh et al. [11] have carried out experimental studies to get the fundamental data for an enhanced mist-cooled heat exchanger. These studies have largely improved the understanding of the air/water mist flow heat transfer enhancement mechanism. However, they failed to estimate the sufficient relation between the heat transfer rate and a range of relevant parameters of the heated surface located in downstream rows of heat exchange devices.

Objectives and scientific relevance

The paper presents a developed air/water mist cooling scheme featuring an ultrasonic mist generator and three copper spheres used as heated surfaces under constant heat flux. The main objective is to clarify the effect of suspending fine water droplets (mist) have on the cooling process and predict the heat transfer rate, friction factor, and thermal performance behaviors for both upstream and downstream heated rows at various water mist rate (j = 23.39–111.68 kg m^{-2} hr^{-1}) and Re range of 2500 < Re <55 000. Such experiment shall help to understand the forced convection cooling process, considered important in engineering and industrial applications including passive heat removable systems in nuclear power plants, heat exchanger models, electrical and electronic devices and so on.

1. Heat transfer enhancement with air/water mist flow

The air/water mist technique is effected by injecting minimum-sized water droplets in the main air flow. Using air/water mist flow as working medium provides an excellent technique of heat transfer enhancement and allows for a significant reduction in size and weight of heat exchanger modules. It also has huge potential for high-heat-flux thermal management due to the high thermal properties of air/water mist mixture if compared to pure air. When the target surface temperature is very high, the water mist can be fully evaporated before it reaches the heated surface due to the force of evaporation. At low surface temperature, the water mist can wet the heated surface, covering it with a water film. The key factors of air/water mist-cooling technique used to enhance the heat transfer process compared to single phase air-cooling can be outlined as follows: a large amount of energy is absorbed in the form of latent heat during the evaporation process, thus, the water particles work as numerous and active heat sinks in the heated surface; the heat capacity of the mixture increases along with the turbulence in the air-side and inside the boundary layer [12].

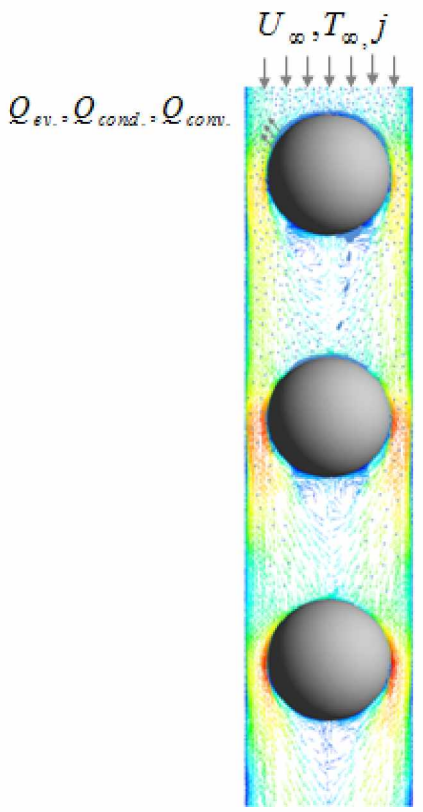

Fig. 1. The surface configuration and mist direction in tandem arrangement

This mist flow regime appears to be appropriate only for the upstream heated surface where water mist impinges actively. Therefore, one should focus on the water mist behavior on the heat transfer surfaces located downstream, and the mode of heat transfer process on the lower heating surface rows. Although the water mist particles carried with the main air flow are caught by the surface of the upstream row, the impinging mist rate is extremely small. However, some water particles may be expected to fall from the upper heating surface. Fig. 1 shows the instantaneous velocity vector maps made by CFD simulation and the direct observation of the surface configuration and mist direction for the tandem arrangement of the heated sphere rows. Basically, the heat transfer mechanism for each sphere row may include three important physical parts: convection (Q_{con}), conductive (Q_{cond}) heat transfer and evaporation of water particles (mist) on the heating surface (Q_{ev}) [13]:

$$Q = Q_{con} + Q_{cond} + Q_{ev}. \quad (1)$$

2. Experimental arrangement and methodology

Fig. 2 schematically presents the experimental installation used to simulate the air/water mist heat transfer process. The experimental facility mainly consists of an adiabatic vertically-set channel with a circular cross-section of 50 mm outer diameter, 3 mm-thick walls and 940 mm total length.

Air was pumped by using 1000 W air blower with AC voltage regulator to adjust airflow velocity. On the same axis, a compact pitot-tube with digital manometer was used to measure the mean flow velocity. The test objects are copper calorimetric spheres, 34 mm in diameter, packed inside the channel in tandem arrangement with constant pitch ratio (y/d = 1). The test spheres were independently heated using 100 W electrical heater having 8 mm-diameter and 31 mm-length. Two k – type calibrated thermocouples were used for each sphere to directly measure the surface temperature tapped in positions as shown in Fig. 3. The inlet and outlet fluid temperatures were recorded using two thermocouples placed immediately upstream and downstream of the channel. All thermocouples were connected to a data acquisition system that consisted of an analog input module type OWEN MV110-8A with MSD200 data logger. All thermocouples, the temperature recorder, and pitot-tube had been calibrated prior to the experiment. The air/water mist was produced by blending fine water droplets (~ 3 μm) into air coolant. To blend the water mist supplied from the mist subsystem with a controlled amount of air, a mixing chamber was installed and used as a blender. The water mist subsystem was a 1.7 MHz ultrasonic mist generator consisting of a piezoelectric transducer, water tank, and a blower fan. This type of mist generator was selected due to the low power consumption and a very quiet operation, compared to other mist and evaporative generators. Manometric fluid with specific density 0.95 was used in inclined manometer to ensure the accurate measurement of the pressure drop across an array of spheres at a range of Reynolds numbers.

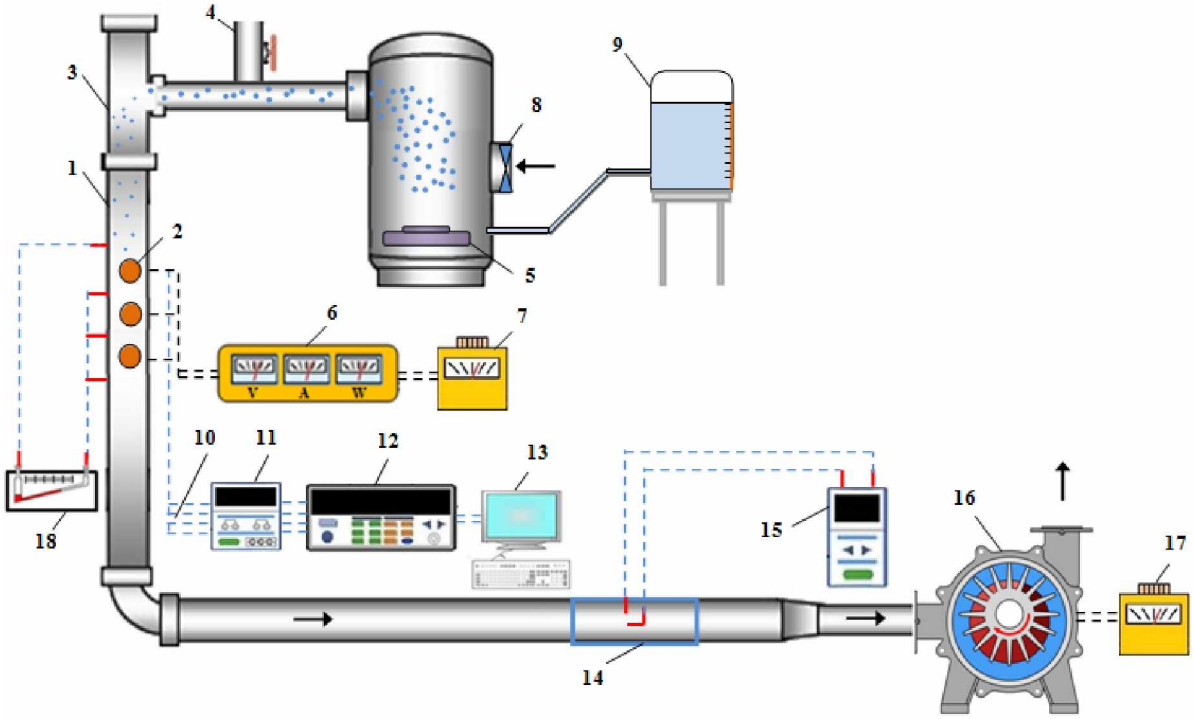

Fig. 2. Schematic diagram of the experimental Set-Up: 1 – Adiabatic channel; 2 – Copper sphere; 3 – Mixing chamber; 4 – Control valve; 5 – Mist generator; 6 – Multimeter; 7, 17 – Voltage regulator; 8 – Fan; 9 – Water tank; 10 – Thermocouples; 11 – Analog signal input; 12 – Data logger; 13 – Computer; 14 – Pitot tube; 15 – Digital manometer; 16 – Air blower; 18 – Inclined manometer

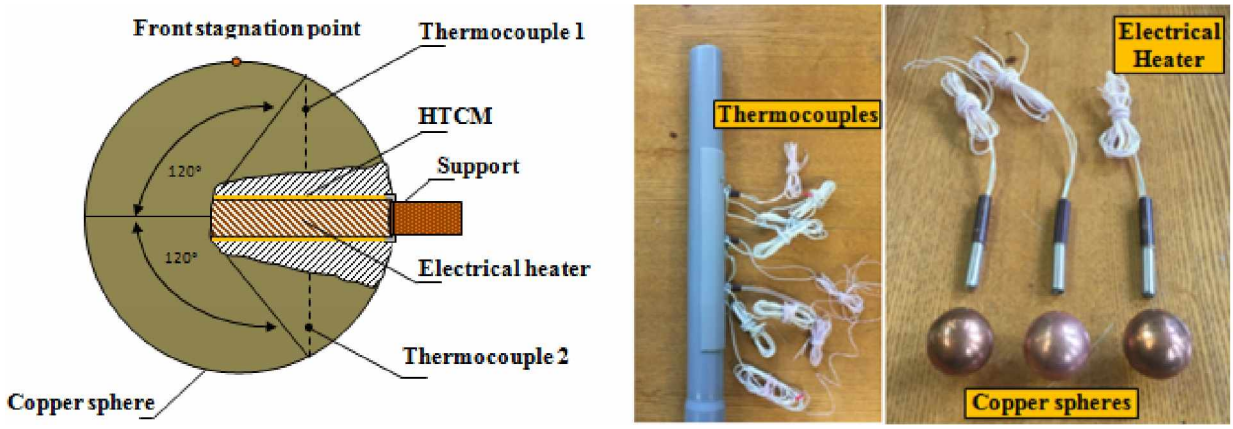

Fig. 3. Heat transfer model

3. Data Reduction and Uncertainty Analysis

In the course of the study, the water droplet diameter was determined based on the capillary wave mechanism using Lang formula (2) [14]:

$$d_p = 0.34\left(\frac{8\pi\sigma}{\rho F^2}\right)^{1/3}, \qquad (2)$$

where σ is the surface tension coefficient and F – the working frequency of the ultrasonic mist generator. When analyzing the interaction of heated surface with air/water mist mixture, the equation in the form of total heat carried by the mixture and heat of water droplets evaporation is usually considered [15]:

$$m_k C_{p,k}\frac{dT}{dt} = \alpha\ F\left[\left(T_s - T_i\right) + h_{fg}\frac{dm_p}{dt}\right]; \qquad (3)$$

$$\frac{dm_p}{dt} = -\beta_m F(X_s - X_i), \qquad (4)$$

where α is the air/water mist heat transfer coefficient, F – surface area, $T_s - T_i$ – surface temperature and input mixture temperature, h_{fg} – the latent heat of evaporation, β – mass transfer coefficient, $X_s - X_i$ – moisture content of saturated air by temperature $T_s - T_i$. Equation (3) can be written as

$$Q = \alpha F\left[\left(T_s - T_i\right) + \frac{h_{fg}}{C_p}\left(X_s - X_i\right)\right]. \quad (5)$$

The relative Reynolds number (Re) can be defined as

$$\mathrm{Re} = \frac{UD\rho}{\mu}. \quad (6)$$

The friction factor is obtained by Darcy – Weisbach equation (6) [16]:

$$f = \frac{2\Delta P}{N\rho U^2}. \quad (7)$$

The heat transfer performance factor can be defined as the ratio of the heat transfer coefficient of air/water mist flow to that of a single phase flow at constant pumping power. It can be written as (8) [17]:

$$\eta = \frac{\alpha_m}{\alpha_a} = \frac{\mathrm{Nu}_m}{\mathrm{Nu}_a} = \left(\frac{\mathrm{Nu}_m}{\mathrm{Nu}_a}\right)\left(\frac{f_m}{f_a}\right)^{-1/3}. \quad (8)$$

The reliability of experimental facility has been evaluated by determining the uncertainties of experimental results [18]. The uncertainties of non-dimensional parameters were found to be 4%, 1.91%, and 1.8%, for Nusselt number, Reynolds number and friction factor respectively.

4. Results and Discussion

Figs. 4 and 5 present the average temperature for single-phase airflow and the pressure drop across the sphere rows for single-phase and air/water mist flows.

The hydrodynamic characteristics of bluff bodies such as vortex shedding mechanisms and velocity field have also been studied by various researchers [19, 20]. The experimental results show that the turbulence intensity accelerates, forming a vortices shedding in the rear of the sphere depending on the flow velocity, and the pressure drop in the terms of friction factor over the sphere decrease downstream. Fig. 4 indicates the results of the average temperature distribution on the heated rows. In single-phase air flow, the working fluid passed over the front region of sphere. However, in the rear of sphere the flow separated and re-circulated in the near wake region, the turbulence intensity increased rapidly, while the velocity became more fluctuating. Vortices were formed, the flow became wavy in structure. That ultimately improved the heat transfer performance and led to an increase in the heat dissipation from the second and third rows. The friction factor in air/water mist flow, as specified with shaded symbols, was found to slightly exceed that in a single-phase air flow – about 2.8 %, 1.8%, and 1.5% respectively for all heated rows as shown in Fig. 5. In air/water mist flow, the water mist evaporation became significant. It can be seen that the surface temperature decreases for all heated rows as water mist rate increased as shown in Fig. 6. These results suggest that suspending water mist in the main air flow is a very efficient thermal management means. The average surface temperature on the first heated row decreased extremely along with the increase in the water mist rate (*j*) due to the thin water film wetting that occurred in high water mist rate and Reynolds number (Re > 17 500). It led to the improved heat transfer due to the latent evaporation heat release.

In the second and third rows, the improvement of heat transfer process depended on the presence or absence of the water mist is. Higher air velocity can force more water mist to approach the downstream heated surfaces, thus enhancing the heat transfer rate. The surface temperature decreased about 52%, 23%, and 13% respectively for all heated rows compared with the single phase airflow under 111.68 kg m^{-2} hr^{-1} water mist rate. The heat transfer coefficient of a single phase airflow in tandem arrangement of heated surfaces also depended on the geometry and flow structure. Fig. 7 shows the experimental results for the average heat transfer coefficient as a function of the number of heated rows for a range of Reynolds number. In air/water mist flow the results of average

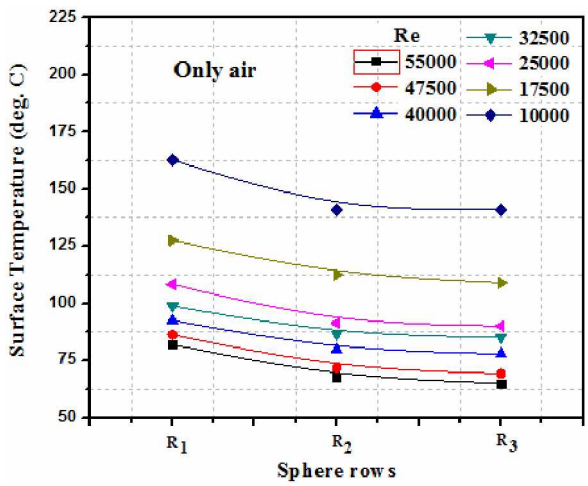

Fig. 4. Variations of surface temperature of sphere rows under various Re number

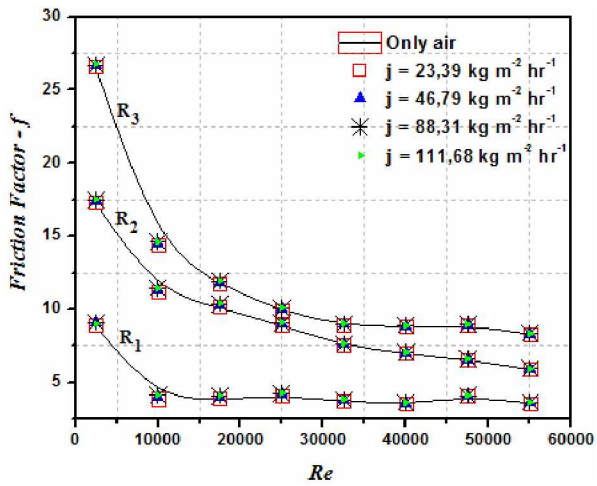

Fig. 5. Variations of friction factor with Re number under different of water mist rate

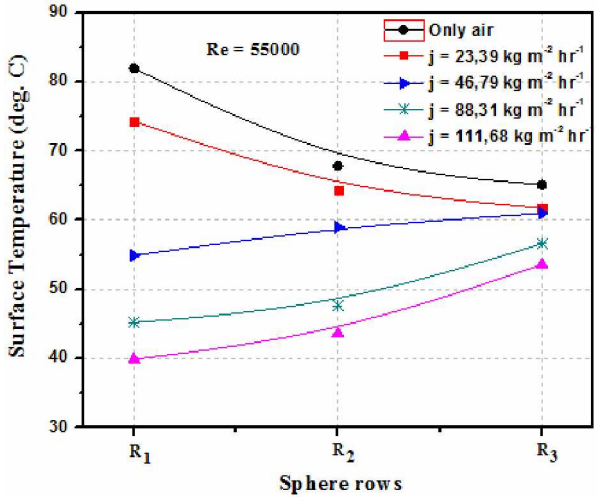

Fig. 6. Variations of surface temperature of sphere rows with different water mist rates

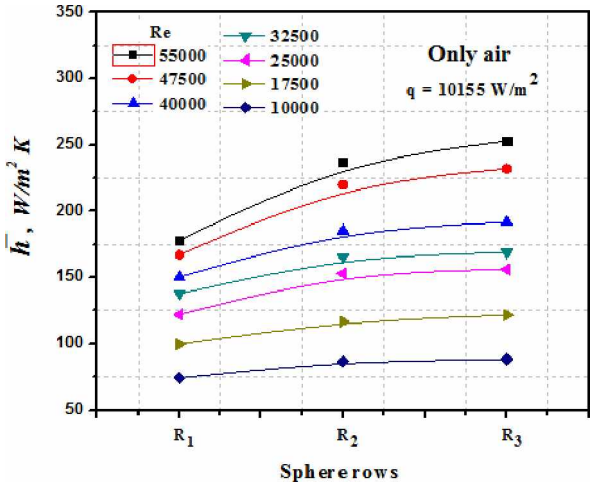

Fig. 7. Variations of heat transfer coefficient of sphere rows under various Re

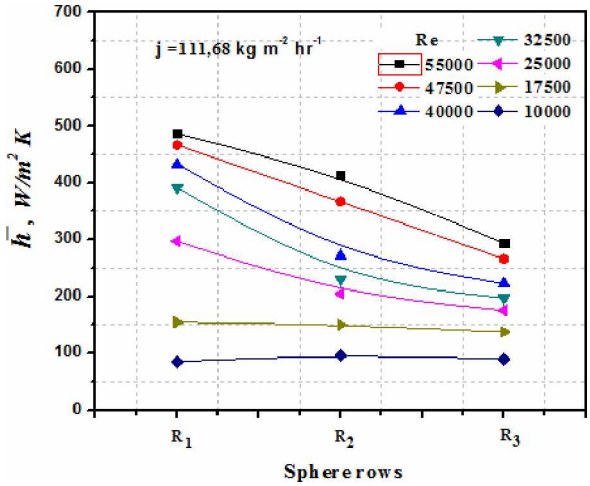

Fig. 8. Variations of heat transfer coefficient of sphere rows under different of water mist rate

heat transfer coefficient in the cross-section under 111.68 kg m^{-2} hr^{-1} of water mist rate is shown in Fig. 8. It shows that the average heat transfer coefficient significantly increased as the Reynolds number increased under constant water mist rate. The upstream row always acted similarly to the single heated row but in the downstream rows, since the water mist carried with the air main flow were caught by the sphere of the upstream row, the impinging water mist rate is extremely small, but downfall water droplets from the upper row must be expected. Thus, the heat transfer coefficient of the lowest of the second and third rows increase was different from that of the upper ones. For the Reynolds number range (Re = 55 000), the average heat transfer coefficient of air/water mist flow for all sphere rows was 170%, 75%, and 17% respectively higher than those in the single phase for (j =111.68 kg m^{-2} hr^{-1}).

Figs. 9, 10, and 11 depict the heat transfer enhancement factor with Reynolds number under the water mist rate range. For the upstream sphere, it was obviously that the heat transfer performance for all cases of water mist rate were generally more than unity and that indicates the impact of suspending water mist into air main flow on the heat transfer process. For Reynolds number range (Re = 2500–10 000), the enhancement factor was in a range between 1.0–1.15 for all the cases of the water mist rate. The suggested explanation is that when the surface temperature is very high, the water mist can be completely evaporated before reaching the heated surface due to the force of evaporation, and not wet the heated surface.

Then, the enhancement factor rapidly increased along with the increase of Reynolds number values (Re > 17 500). At Reynolds number range (Re = 40 000), the enhancement factor was 2.87 of that with single phase air cooling for the water mist rate (111.68 kg m^{-2} hr^{-1}). For the downstream of the second and the third rows, the pattern of heat transfer performance increase was different from that of the upper ones. The heat transfer

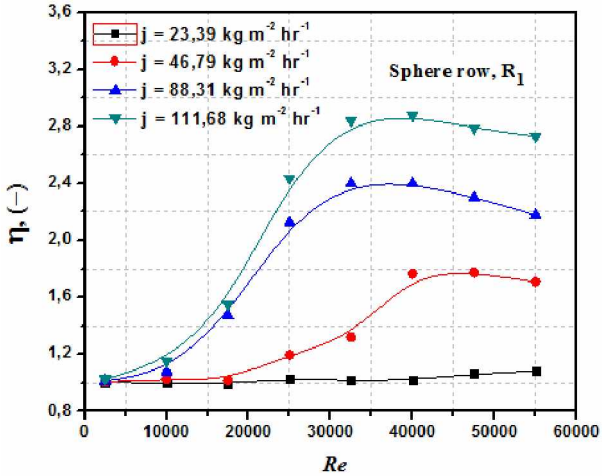

Fig. 9. Variations of heat transfer performance factor with Reynolds number for upstream row (R_1) under the range of the water mist rate

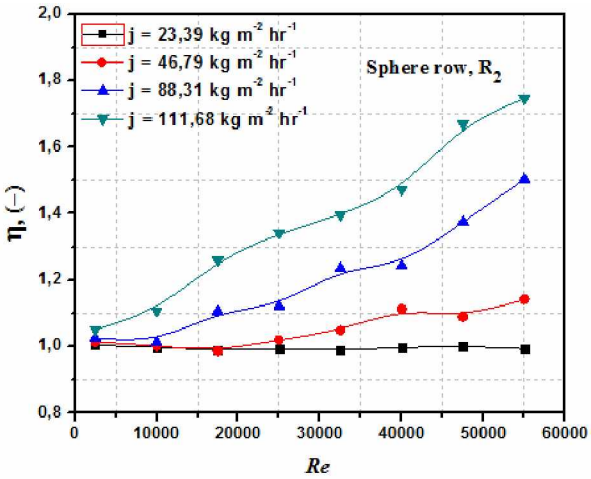

Fig. 10. Variations of heat transfer performance factor with Reynolds number for second row (R_2) under the range of the water mist rate

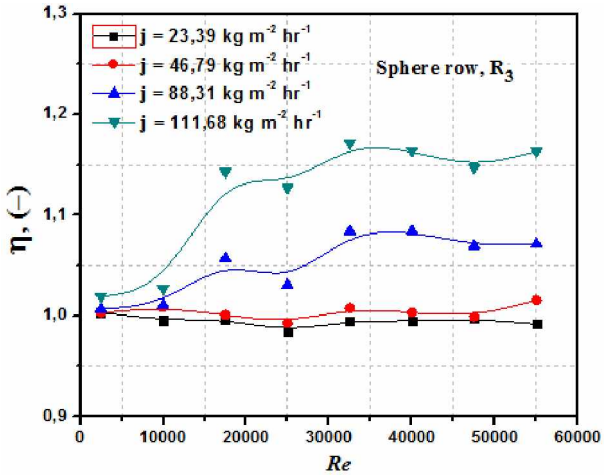

Fig. 11. Variations of heat transfer performance factor with Reynolds number for third row (R_3) under range of water mist rate

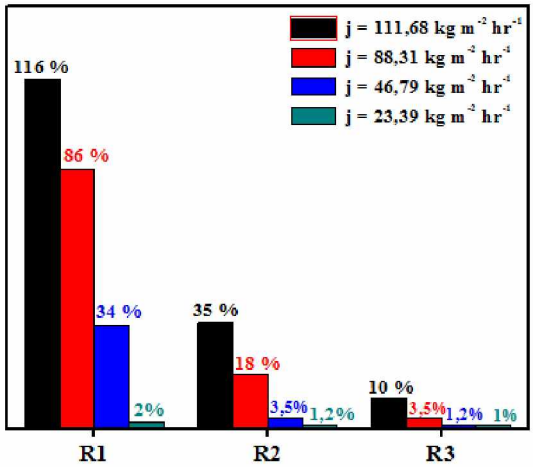

Fig. 12. Percentage of heated rows enhancing performance

performance increased linearly with the increase in the Reynolds number but depended on the water mist content.

The vapor cooling mechanism may occur as a result of the mist evaporation in upstream row and the residual water mist. At Reynolds number range (Re = 55 000), the enhancement factor for second and third rows was 1.74 and 1.16 times of that with the single phase air cooling for water mist rate (111.68 kg m^{-2} hr^{-1}). The cooling of the heated surfaces was most affected by the presence of the water mist. Fig. 12 presents the percentage enhancement in the overall thermal performance for all heated rows.

Conclusion

This experimental study investigated the influence of the suspended water mist on the heat transfer characteristics in tandem arrangement of spheres packed inside cylindrical channel in the open air/water mist system for the range of Reynolds numbers $2500 \le Re \le 55\,000$. The presence of water mist with different rates provided for a more efficient heat transfer enhancement compared to the single phase – air cooling. The surface temperature decreased by about 52%, 23%, and 13% respectively for all heated rows under (111.68 kg m^{-2} hr^{-1}) water mist rate. The pressure drop in the term of friction factor was found to slightly exceed that generated by single-phase air flow for about 2.8%, 1.8%, and 1.5% respectively for all the heated rows. For the upper sphere, the average heat transfer performance was found to be 116%, 35%, and 10% of that with single phase air cooling for the water mist rate (111.68 kg m^{-2} hr^{-1}). For the lower spheres of the second and third rows, the heat transfer performance factors were 1.74 and 1.16 times for the water mist rate (111.68 kg m^{-2} hr^{-1}) and Reynolds number (Re = 55 000).

References

1. Hayashi Y., Takimoto A., Matsuda O. and Kitagawa T. Study on Mist Cooling for Heat Exchanger: Development of High-Performance Mist-Cooled Heat Transfer Tubes. *JSME International Journal. Ser. 2, Fluids Engineering, Heat Transfer, Power, Combustion, Thermophysical Properties*, 1990, vol. 33, no. 2, pp. 333–339. DOI: 10.1299/jsmeb1988.33.2_333

2. Hayashi Y., Takimoto A. and Matsuda O. Heat Transfer from Tubes in Mist Flows. *Experimental Heat Transfer*, 1991, vol. 4, no. 4, pp. 291–308. DOI: 10.1080/08916159108946422

3. Lee S., Park J., Lee P. and Kim M. Heat Transfer Characteristics during Mist Cooling on a Heated Cylinder. *Heat Transfer Engineering*, 2005, vol. 26, no. 8, pp. 24–31. DOI: 10.1080/01457630591003718

4. Kosky P. Heat Transfer to Saturated mist Flowing Normally to a Heated Cylinder. *International Journal of Heat and Mass Transfer*, 1976, vol. 19, no. 5, pp. 539–543. DOI: 10.1016/0017-9310(76)90167-8

5. Kuwahara H., Nakayama W. and Mori Y. Heat Transfer from the Heated Cylinders with Various Surfaces in Air/Water Mist Flows. *Heat Transfer Res.*, 1981, vol. 10, pp. 119.

6. Allais I., Alvarez G. and Flick D. Modelling Cooling Kinetics of a Stack of Spheres during Mist Chilling. *Journal of Food Engineering*, 2006, vol. 72, no. 2, pp. 197–209. DOI: 10.1016/j.jfoodeng.2004.11.010

7. Allais I. and Alvarez G. Analysis of Heat Transfer during Mist Chilling of a Packed Bed of Spheres Simulating Foodstuffs. *Journal of Food Engineering*, 2001, vol. 49, no. 1, pp. 37–47. DOI: 10.1016/S0260-8774(00)00182-5

8. Wen-Jei Y. and Clark D. Spray Cooling of Air-Cooled Compact Heat Exchangers. *International Journal of Heat and Mass Transfer*, 1975, vol. 18, no. 2, pp. 311–317. DOI: 10.1016/0017-9310(75)90162-3

9. Treble, M. An Approximate Calculation of Heat Transfer during Flow of an Air-Water Mist along a Heated Flat Plate. *International Journal of Heat and Mass Transfer*, 1981, vol.24, no.4, pp. 749–755. DOI: 10.1016/0017-9310(81)90018-1

10. Song C.H., Lee D.Y., and Ro S.T. Cooling Enhancement in an Air-Cooled Finned Heat Exchanger by Thin Water Film Evaporation. *International Journal of Heat and Mass Transfer*, 2003, vol. 46, no. 7, pp. 1241–1249. DOI: 10.1016/S0017-9310(02)00405-2

11. Deshmukh A. Design, Development and Fabrication of a Mist Spray Direct Evaporative Cooling System and Its Performance Evaluation. *Journal of Thermal Engineering*, 2019, pp. 42–50. DOI: 10.18186/thermal.513053

12. Wang T. and Dhanasekaran T. Calibration of a Computational Model to Predict Mist/Steam Impinging Jets Cooling With an Application to Gas Turbine Blades. *Journal of Heat Transfer*, 2010, vol. 132, no. 122201. DOI: 10.1115/1.4002394

13. Bian Q., Wang J., Chen Y., Wang Q. and Zeng M. Numerical Investigation of Mist/Air Impingement Cooling on Ribbed Blade Leading-Edge Surface. *Journal of Environmental Management*, 2017, vol. 203, pp. 1062–1071. DOI: 10.1016/j.jenvman.2017.05.052

14. Kudo T., Sekiguchi K., Sankoda K., Namiki N. and Nii S. Effect of Ultrasonic Frequency on Size Distributions of Nanosized Mist Generated by Ultrasonic Atomization. *Ultrasonics Sonochemistry*, 2017, vol. 37, pp. 16–22. DOI: 10.1016/j.ultsonch.2016.12.019

15. Kumari N., Bahadur V., Hodes M., Salamon T., Kolodner P., Lyons A. and Garimella S. Analysis of Evaporating Mist Flow for Enhanced Convective Heat Transfer. *International Journal of Heat and Mass Transfer*, 2010, vol. 53, pp. 3346–3356. DOI: 10.1016/j.ijheatmasstransfer.2010.02.027

16. Jiang G., Shi X., Chen G. and Gao J. Study on Flow and Heat Transfer Characteristics of the Mist/Steam Two-Phase Flow in Rectangular Channels with 60 deg. Ribs. *International Journal of Heat and Mass Transfer*, 2018, vol. 120, pp. 1101–1117. DOI: 10.1016/j.ijheatmasstransfer.2017.12.082

17. Manglik R. and Bergles A. Fully Developed Laminar Heat Transfer in Circular-Segment Ducts with Uniform Wall Temperature. *Numerical Heat Transfer*, 1994, Part A: Applications, vol. 26, no. 5, pp. 499–519. DOI: 10.1080/10407789408956006

18. Kline S.J. and McClintock F.A. Describing Uncertainties in Single-Sample Experiments. *Mechanical Engineering*, 1953, vol. 75, no. 1, pp. 3–8.

19. Abed A. and Shcheklein S. Investigation of Hydrodynamic Characteristics of Laminar Flow Condition Around Sphere Using PIV System. *Journal of Physics: Conference Series*, 2018, vol. 1015, no. 032001. DOI: 10.1088/1742-6596/1015/3/032001

20. Kotsev T. Viscous Flow Around Spherical Particles in Different Arrangements. *MATEC Web of Conferences*, 2008, vol. 145, no. 03008. DOI: 10.1051/matecconf/201814503008

Received 7 March 2019

УДК 536.24
DOI: 10.14529/power190202

ЭКСПЕРИМЕНТАЛЬНОЕ ИССЛЕДОВАНИЕ ГИДРОДИНАМИКИ И ТЕПЛООБМЕНА В ЭМУЛЬСИОННОМ РЕЖИМЕ ТЕЧЕНИЯ ДВУХФАЗНОГО ПОТОКА «ГАЗ – ЖИДКОСТЬ» ПРИ ТАНДЕМНОМ РАСПОЛОЖЕНИИ НАГРЕТЫХ СФЕР

Ахрам Х. Абед[1, 2], С.Э. Щеклеин[1], В.М. Пахалуев[1]

[1] Уральский федеральный университет им. первого Президента России Б.Н. Ельцина, г. Екатеринбург, Россия,
[2] Технологический университет, г. Багдад, Ирак

Проведено экспериментальное исследование гидродинамики и теплообмена нагреваемых рядов, тандемно расположенных в цилиндрическом канале с воздушным, а также воздушно-водным эмульсионным режимом течения в качестве рабочей среды. Средняя температура на поверхности регистрировалась при разных значениях основного воздушного течения, скорости течения водяного тумана, теплового потока при постоянном шаговом отношении (y/d = const). Обнаружилось, что интенсивность теплообмена повышается со скоростью течения водяного тумана и понижается с температурой поверхности. Теплообмен усилился по сравнению с однофазным воздушным потоком за счет испарения водяного тумана и прямого проведения тепла водяной пленкой, формирующейся на нагреваемых поверхностях. В целом коэффициент теплообмена удалось повысить примерно на 140, 42 и 10 % в верхнем, среднем и нижнем нагреваемых рядах, соответственно, за счет суспенирования водяного тумана со скоростью потока 111,68 кг·м$^{-2}$·ч$^{-1}$. По сравнению с другими значениями скорости в исследуемом диапазоне коэффициент теплообмена повысился на 116, 35 и 10 % соответственно по всем нагреваемым рядам при наибольшем значении скорости. Полученные результаты могут быть полезны при разработке новых конструктивных решений модулей теплообмена.

Ключевые слова: экспериментальное исследование, эмульсионный режим, усиление теплообмена, тандемное расположение, водяная пленка.

Абед Акрам Хамзах, аспирант, Уральский федеральный университет им. первого Президента России Б.Н. Ельцина, г. Екатеринбург; Технологический университет, г. Багдад, Ирак; akraaam82@yahoo.com.

Щеклеин Сергей Евгеньевич, д-р техн. наук, профессор, заведующий кафедрой «Атомные станции и возобновляемые источники энергии», Уральский федеральный университет им. первого Президента России Б.Н. Ельцина, г. Екатеринбург; s.e.shcheklein@urfu.ru.

Пахалуев Валерий Максимович, д-р техн. наук, профессор, кафедра «Атомные станции и возобновляемые источники энергии», Уральский федеральный университет им. первого Президента России Б.Н. Ельцина, г. Екатеринбург; valer-1939@mail.ru.

Поступила в редакцию 7 марта 2019 г.

ОБРАЗЕЦ ЦИТИРОВАНИЯ

Abed, Akram H. Experimental Investigation of Hydrodynamics and Heat Transfer Characteristics of Two-Phase Gas/Liquid Mist Flow in Tandem Arranged Heated Spheres / Akram H. Abed, S.E. Shcheklein, V.M. Pakhaluev // Вестник ЮУрГУ. Серия «Энергетика». – 2019. – Т. 19, № 2. – С. 14–21. DOI: 10.14529/power190202

FOR CITATION

Abed Akram H., Shcheklein S.E., Pakhaluev V.M. Experimental Investigation of Hydrodynamics and Heat Transfer Characteristics of Two-Phase Gas/Liquid Mist Flow in Tandem Arranged Heated Spheres. *Bulletin of the South Ural State University. Ser. Power Engineering*, 2019, vol. 19, no. 2, pp. 14–21. DOI: 10.14529/power190202